Raman spectroelectrochemical determination of clopyralid in tap water

Martin Perez-Estebanez [*], William Cheuquepan, Maria Huidobro, Jose Vicente Cuevas, Sheila Hernandez, Aranzazu Heras, Alvaro Colina [*]

Department of Chemistry, Universidad de Burgos, Pza. Misael Bañuelos s/n, E-09001 Burgos, Spain

ARTICLE INFO

ABSTRACT

Clopyralid is a common herbicide used all around the world that can be dissolved in the rain stream and accumulate in underground water with the potential threat of reaching drinking water. Many methodologies have been proposed to perform quantitative analysis of this compound but, to this day, no Raman detection of clopyralid has been carried out. Here, a novel methodology to quantify clopyralid, based on *Electrochemical Surface Oxidation-Enhanced Raman Scattering* (EC-SOERS), is developed, using disposable silver screen-printed electrodes as substrate. The optimization of the electrolytic media is carried out, searching for the conditions where a maximum Raman enhancement is obtained. Moreover, a study about the effect of various interfering compounds, which could be present in water, on the clopyralid Raman response is performed. The results demonstrate that the presented methodology allows the determination of clopyralid in the micromolar range in tap water without any purification or preconcentration step, requiring few minutes to perform the measurement of each sample.

1. Introduction

Herbicides and pesticides are substances that play a key role in modern society since they allow us to maximize the efficiency of our cropping system. However, the extensive usage of these compounds can lead to numerous problems, such as the contamination of water or soils.

Clopyralid is a common organochlorine herbicide, from the family of pyridine carboxylic acids. It is used all around the world to prevent the growth of perennial broad-leaf weeds. As an auxin-mimic, its mechanism of action is related with its ability to emulate the hormone auxin, disrupting the growing process of plants [1]. Clopyralid is a highly soluble herbicide with low affinity to most kinds of soils, resulting in a low retention time [2]. In addition to that, the main mechanism of degeneration of this specie is due to microbial metabolism [3], which is considered a slow process for the degradation of herbicides. This combination of factors allows the accumulation of clopyralid in rivers and underground streams, due to the transport of clopyralid dissolved by rain. This is a problem that persists today, and in fact, a few years ago a study performed in Ireland revealed the presence of clopyralid in drinking water with concentration above the recommended levels of the EU for this kind of compounds [4]. For these reasons, the development of methodologies for the detection and quantification of clopyralid and other herbicides is key for the control and regulation of these compounds.

Some methodologies has been reported in literature for the detection of clopyralid, based for example on electrochemiluminescence [5,6] or voltammetric detection [7]. However, the most reported method for the detection of this compound is chromatography, mainly liquid chromatography coupled with mass spectrometry (LC-MS) [4,8,9], tandem mass spectrometry (LC-MS/MS) [10] or gas chromatography coupled with mass spectrometry [11]. Although these techniques are really powerful for analysis, they usually involve tedious pretreatment samples, expensive equipment and long analysis time.

Raman spectroscopy is a spectroscopic technique that has gained relevance during the last years for quantitative analysis [12]. Although this technique has always suffered a lack of sensitivity due to the low analytical signal given by Raman scattering, the discovery of Raman enhancement phenomena, starting with *Surface-Enhanced Raman Scattering* (SERS) by Fleishman *et al.* [13], broadened the applications of Raman spectroscopy. SERS is a phenomenon capable of enhancing the Raman signal of molecules up to 10^{10} times [14–16], and its origin is related to various mechanisms. The principal factor to achieve the Raman enhancement is called the electromagnetic mechanism (EM). The EM is related with the localized surface plasmon resonance of the metallic nanostructures that conform SERS substrates, and with the influence of this resonance on the electric field surrounding those

---

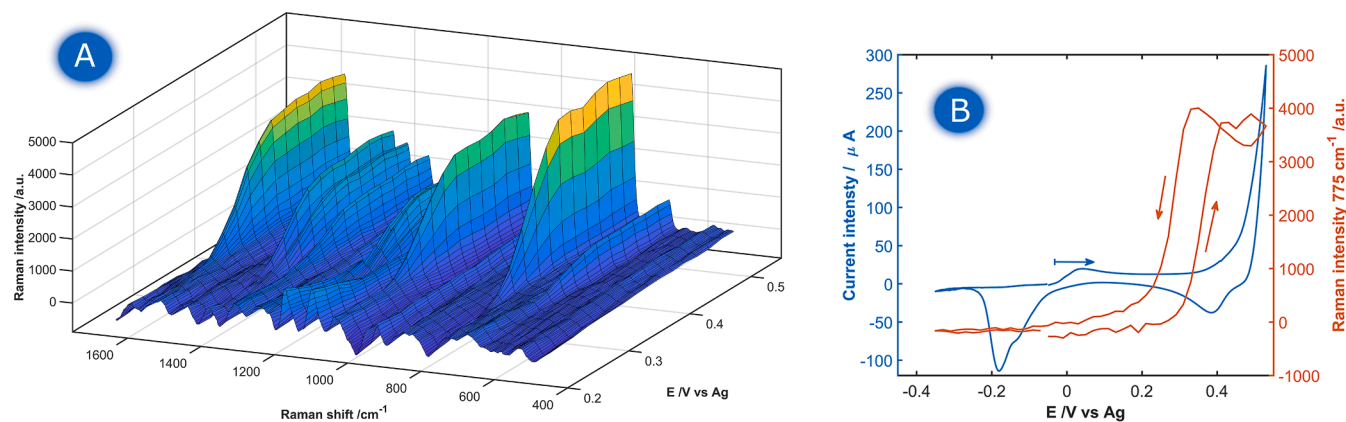**Fig. 1.** (A) 3D Surface plot of the evolution of Raman signal of Clopyralid during the first oxidation sweep of a AgSPE. (B) CV and VoltaRamangram at 775 cm^{-1} during a complete voltammetry cycle. (A) and (B) figures corresponds to the same experiment. Electrolytic conditions: HClO$_4$ 0.1 M + KBr 5 mM + clopyralid 90 μM.

structures. The enhanced electric field generated during this resonance can modify the polarizability of the molecules close to the nano-structures [17–19], enhancing its Raman activity up to 10^9 [15,20–22]. The second factor which controls the Raman enhancement is called the chemical mechanism (CM), and it is related to a number of processes that promote a charge transfer between the SERS substrate and the adsorbed analyte [21,23]. Generally, it is considered that the CM generates lower Raman enhancements than the EM. Theoretical studies showed in the past that chemical enhancement should have a theoretical limit of 10^3 for pyridine interacting with silver clusters [15], but most experimental studies showed enhancement factors of one or two orders of magnitude related with CM [21,24]. Only some recent studies with semiconductor materials has shown that CM can yield enhancement factors over 10^3 [25].

Although SERS is a powerful technique for the analysis of a big number of species [26], the power of the technique can be further improved by coupling Raman spectroscopy with electrochemistry [12]. The combination of these techniques can help to modulate the morphological properties of the SERS substrate [17,27] and/or promote the adsorption of species over the substrate or modulate its geometry [28], improving the sensitivity of the technique. The use of Raman spectroelectrochemistry has allowed the development of new strategies to enhance the Raman signal of molecules, such as *Electrochemical Surface Oxidation-Enhanced Raman Scattering* (EC-SOERS). This phenomenon was first reported a few years ago [29], and allows the enhancement of the Raman signal of certain molecules during the electrochemical oxidation of a silver electrode. EC-SOERS has proven to be especially selective for molecules containing carbonyl and/or carboxyl groups, which gives the method a great selectivity for analytes with those functional groups [30–32].

In this work, we present a new methodology based on the EC-SOERS phenomenon for the quantitative detection of clopyralid in water samples using silver screen-printed electrodes (AgSPE) as disposable substrates. To the best of our knowledge, this is the first time that a methodology for clopyralid detection using Raman spectroscopy techniques has been developed.

2. Methods and materials

2.1. Reagents and solutions

Perchloric acid (HClO$_4$, 60 %, Sigma-Aldrich), potassium chloride (KCl, 99 %, ACROS Organics), potassium bromide (KBr, 99 %, ACROS Organics), Clopyralid (3,6-Dichloro-2-pyridinecarboxylic acid, >98.0 %, Tokio Chemical Industry), 2,4-D (2,4-dichlorofenoxiacetic acid, 97 %, Sigma-Aldrich), picloram (4-amino-3,5,6-tricloropicolinic acid, 97+%, Sigma-Aldrich). Reagents were used as received, without further

purification. All solutions were prepared using ultrapure water obtained from a Milli-Q® Direct Water Purification System provided by Millipore (18.2 MΩ·cm resistivity at 25 °C, TOC value of 2 ppb). In this work, the test sample was prepared in ordinary tap water instead of ultrapure water.

2.2. Instrumentation

In-situ time-resolved Raman spectroelectrochemistry (TR-Raman-*SEC*) was performed with a customized SPELEC-RAMAN instrument (Metrohm-DropSens), which includes a 785 nm laser source. The laser power in all experiments was set at 80 mW (254 W cm^{-2}). This instrument was connected to a Raman probe (DRP-RAMANPROBE, Metrohm-DropSens). A home-made cell for screen-printed electrodes was used during the experiments. DropView SPELEC software (Metrohm-DropSens) was used to control the instrument, which allows getting real-time and synchronized spectroelectrochemical data. An integration time of 1 s was used for all the TR-Raman-*SEC* experiments. AgSPE from Metrohm DropSens (DRP-C013) were used as electrochemical set-up. These electrodes consist of a working electrode of silver with a diameter of 1.6 mm, a carbon counter electrode and a silver pseudo-reference electrode.

Cyclic voltammetry was used as electrochemical technique to perform TR-Raman-*SEC* experiments. All potentials are referred to the pseudo-reference electrode of silver. For all the samples of the calibration curve, a pretreatment of the electrode surface based on two voltammetric cycles were performed previously to the determination. A CV was applied between −0.35 V and +0.53 V, starting at −0.05 V in anodic direction for each experiment using a blank solution (HClO$_4$ 0.1 M + KBr 5 mM), to improve the sensitivity and the reproducibility of the measurements. A scan rate of 0.02 V s^{-1} and a step potential of 2 mV were set for all electrochemical measurements. All electrochemical experiments were started at −0.05 V in anodic direction.

2.3. Computational methods

All theoretical calculations were performed using the hybrid functional B3LYP [33,34]. For the description of the atoms, basis def2-SVP [35] were used for all the elements adding pseudopotentials in de description of the silver [36]. The optimization of the structures was carried out without any restriction. A molecule of water interacting with the silver cation was used to complete the coordination sphere of the metal in its interaction with the clopyralid. The software package orca Gaussian 09 has been used for these DFT calculations [37].

Table 1
Raman shift assignments for clopyralid.

Experimental Raman shift (cm^{-1})	Band Assignment
344	ν_{sym} (C$_1$-Cl$_{11}$; C$_4$-Cl$_8$) + γ (C—H) + γ ring
672	s$_{sym}$ (C$_1$-N-C$_3$; C$_4$-C$_5$-C$_6$) + γ (C$_6$-H$_{10}$) + γ (O—H)
775	ν_{sym} (C$_1$-Cl$_{11}$; C$_4$-Cl$_8$) + δ_{sym} (C$_5$-H$_9$ + C$_6$-H$_{10}$) + s (O—C—O)
884	s (C$_6$-C$_1$-N) + s(O—C—O) + δ_{sym} (C$_5$-H$_9$; C$_6$-H$_{10}$)
1056	s$_{asym}$ (N-C$_3$-C$_4$; C$_5$-C$_6$-C$_1$) + δ_{asym} (C$_5$-H$_9$; C$_6$-H$_{10}$)
1156	δ (C$_5$-H$_9$; C$_6$-H$_{10}$) + ν (C$_1$-Cl$_{11}$) +
1171	δ (C$_5$-H$_9$) + δ ring
1254	–
1328	ν_{sym} (N-C$_3$; C$_4$-C$_5$; C$_6$-C$_1$)
1387	ν_{asym} (N-C$_3$; C$_5$-C$_6$) + δ_{asym} (C$_5$-H$_9$; C$_6$-H$_{10}$) + δ (O—C—O)
1425	δ_{sym} (C$_5$-H$_9$; C$_6$-H$_{10}$)
1559	ν_{sym} (C$_1$-C$_6$; C$_3$-C$_4$) + δ (C$_5$-H$_9$; C$_6$-H$_{10}$)
1612	ν_{asym} (C$_1$-N-C$_3$) + ν_{asym} (C$_4$-C$_5$-C$_6$) + δ (C$_5$-H$_9$; C$_6$-H$_{10}$)

ν = *Stretching*; δ = *in-plane bending*; s = *scissoring*; γ = *out of plane bending*; w = *wagging. Subscripts stands for symmetric (sym) and assymetric (asym).*

3. Results and discussion

3.1. EC-SOERS of clopyralid

Fig. 1 shows the spectroelectrochemical response for a 90 µM clopyralid sample obtained during the electrochemical oxidation of a AgSPE. The evolution of the Raman spectra during the experiment, Fig. 1A, demonstrates the capability of the EC-SOERS phenomenon to amplify the Raman signal of clopyralid. The Raman enhancement of clopyralid during the oxidation of the silver electrode can be better observed in Fig. 1B. In this figure, the cyclic voltammogram (CV) is plotted in the left axis (blue line), meanwhile in the right axis (orange line) the evolution of Raman intensity of the band at 775 cm^{-1} during the electrochemical experiment is represented. For simplicity, this evolution of the Raman signal with the potential is denoted as VoltaRamangram. The voltammetry starts at −0.05 V where no electrochemical reaction takes place. Four different electrochemical processes can be observed in the CV. First, the electrogeneration of AgBr on the electrode surface, around +0.05 V. Second, the massive dissolution of the Ag electrode to form Ag$^+$ ions, around +0.45 V. Finally, in the cathodic scan, we can find the reduction of Ag$^+$ ions at +0.40 V and the reduction of the AgBr deposited on the electrode surface at −0.20 V. The voltaRamangram at 775 cm^{-1}, orange line in Fig. 1B, shows the enhancement of the Raman signal up to +0.51 V, concomitantly with the

massive oxidation of the silver electrode, what is defined as EC-SOERS. During the cathodic scan, the Raman signal experiments a second increment during the reduction of the Ag$^+$ ions in solution, reaching its absolute maximum value around +0.35 V. This enhancement is vanished during the backward scan of the potential, around + 0.20 V where no electrochemical process is observed. From + 0.35 V onwards in the forward scan, the Raman bands corresponding to the clopyralid are clearly defined. All the observed Raman bands (Fig. 1B), which correspond to the Raman spectrum of clopyralid, show a similar behavior as the band at 775 cm^{-1}.

To the best of our knowledge, clopyralid Raman spectrum has never been reported in literature. In order to properly characterize the Raman spectra of clopyralid, several DFT calculations were performed in which the theoretical Raman spectra of clopyralid under different coordination environments were computed. A total of 4 different clopyralid configurations were simulated, changing the protonation state of the molecule and proposing 3 different ways of coordination with a silver ion, in order to simulate the interaction with the EC-SOERS substrate. The computed structures are shown in Fig. S1. Once that these structures were optimized, the theoretical Raman spectra were calculated and compared with the experimental results. This comparison was used to generate a tentative assignment of the observed Raman bands, which is shown in Table 1. A more in-depth comparison between the experimental and theoretical spectra is presented in Table S1.

It should be noted that no Raman signal was detected at potentials below +0.10 V. No EC-SERS effect is observed after the reduction of AgBr at −0.20 V. This lack of EC-SERS signal could be related to many factors: (i) the presented methodology is not optimized to generate a good EC-SERS substrate or (ii) the adsorption of clopyralid on the silver substrate generated under these experimental conditions is difficult because of its molecular structure, since there are 2 functional groups (chlorine and carboxylate) that generates steric hindering over the pyridinic nitrogen, which is a functional group with high affinity for silver. This absence of SERS response could be related to the lack of SERS spectrum of clopyralid in literature, demonstrating the interest of EC-SOERS for analysis due to the capability of providing Raman responses of many molecules that are not easily obtained using SERS. In fact, using a classical electrochemical protocol for the generation of a SERS substrates (KCl 0.1 M, with several oxidation–reduction cycles) did not provide a good EC-SERS enhancement for this analyte (Fig. S2).

3.2. EC-SOERS signal optimization

As was reported previously, EC-SOERS is a phenomenon highly dependent on the electrolytic medium. Several studies have
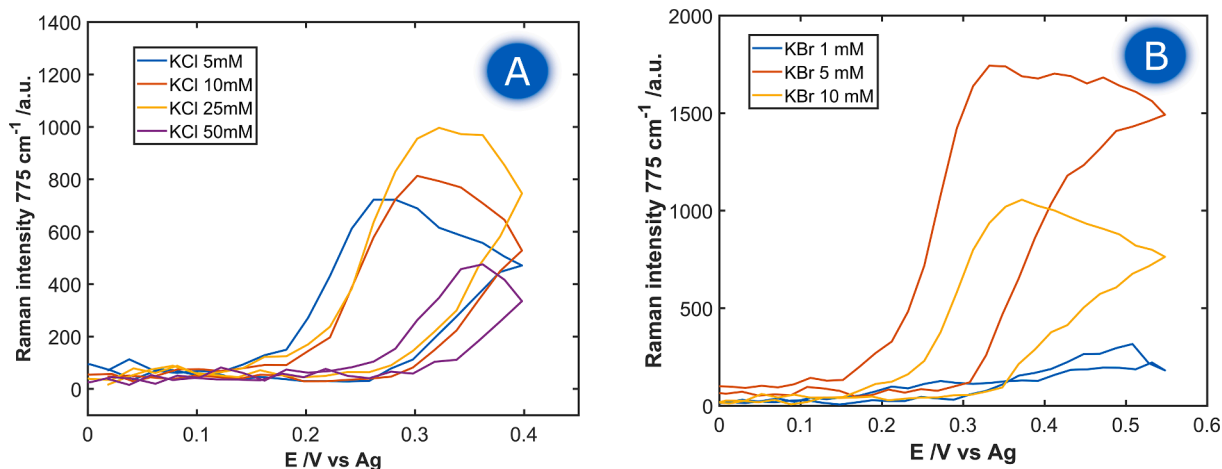
Fig. 2. VoltaRamangrams of clopyralid 100 µM under various electrolytic conditions. All solutions used HClO$_4$ 0.1 M as support electrolyte and had variables concentrations of KCl (A) or KBr (B).
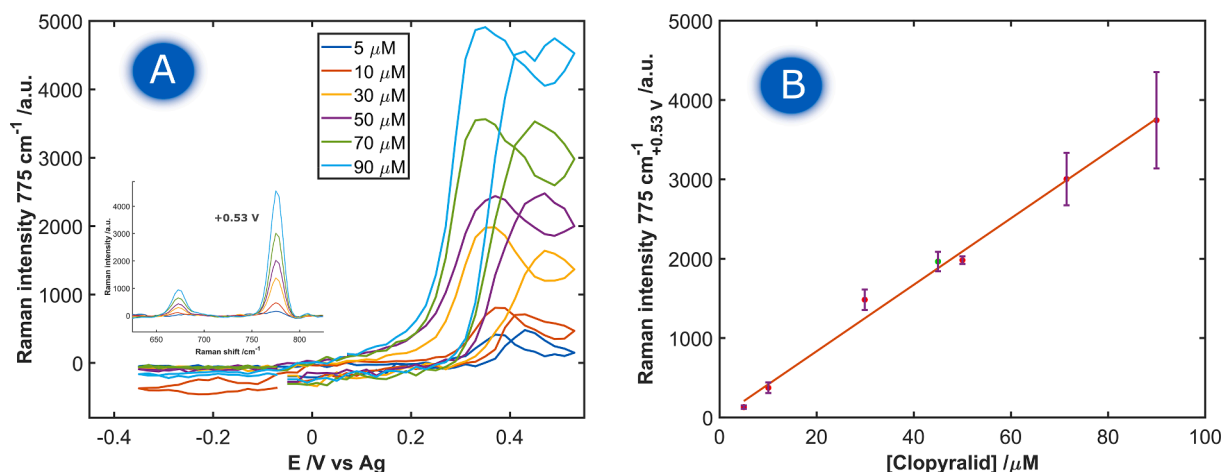
Fig. 3. (A) Evolution of the Raman intensity at 775 cm^{-1} with the potential for various clopyralid concentrations. Inset: detail of the Raman band at 775 cm^{-1} of the different clopyralid concentrations at +0.53 V. (B) Calibration curve using the Raman intensity at +0.53 V. Each sample was measured three times. Green point represents the tap water sample. Electrolytic medium: HClO$_4$ 0.1 M + KBr 5 mM + Clopyralid X μM.

demonstrated the influence on the Raman response of factors like pH, type and concentration of precipitating agent (KCl or KBr) [30,38]. The use of a precipitating agent to generate silver salt crystals is, as far as we know, mandatory to observe the EC-SOERS phenomenon. For this reason, our first step for the optimization of this analytical method was the selection of the best precipitating agent between Cl$^-$ or Br$^-$. With this purpose, the EC-SOERS response of clopyralid under various electrolytic conditions was studied. A summary of the results is presented in Fig. 2. In the case of KCl containing medium (Fig. 2A), the maximum EC-SOERS effect is observed using a 25 mM of KCl. On the contrary, using KBr (Fig. 2B) the maximum Raman enhancement is observed at 5 mM.

The responses for the different concentrations of the precipitating agents can be related to the different solubility product (pKs) of the silver salts, AgCl and AgBr. AgBr, with a higher pKs than AgCl, is a much more effective passivating agent for the silver electrode against anodic dissolution, and because of this, the current associated with the formation of Ag$^+$ is much less prominent for KBr containing media (Fig. S3). Therefore, the applied potential can be further increased in KBr containing media, generating a wider region where EC-SOERS phenomenon can be observed. If the same range of potentials is applied in a KCl containing media, the electrode surface is severely damaged due to the anodic dissolution of silver, reducing the reproducibility of the Raman enhancement.

From the comparison of the voltaRamangrams (Fig. 2) in the different electrolytic conditions can be deduced that the best Raman

response was obtained for a 5 mM KBr solution, obtaining a good sensitivity for clopyralid. These experimental conditions were selected to demonstrate the good analytical performance of EC-SOERS.

3.3. Quantitative analysis

EC-SOERS has proven to be a useful methodology for quantitative analysis [30–32], both in KCl and KBr containing media. Here, a new methodology is used to quantify the presence of clopyralid in water samples. A calibration curve from 5 to 90 μM of clopyralid was prepared, using the optimized electrolytic conditions: 0.1 M HClO$_4$ + 5 mM KBr. For clopyralid concentrations higher than 100 μM, the method loses its linear behavior and the dispersion of the experimental data increases, making easy the detection of clopyralid but difficult the quantification. Thus, samples with a concentration higher than 100 μM have to be diluted for quantification.

Fig. 3A summarizes the data obtained for the calibration curve, showing the voltaRamangram of clopyralid at different concentrations. TR-*SEC*-Raman responses are multivariate by nature, but in simple problems, a univariate analysis of the responses is more than enough to quantify the test molecule, being needed the definition of the best criterion to extract the data from the VoltaRamangrams and assess the corresponding calibration model. Raman intensity of characteristic bands of clopyralid can be extracted at several relevant potentials, for example the maximum of intensity during the cathodic scan or the
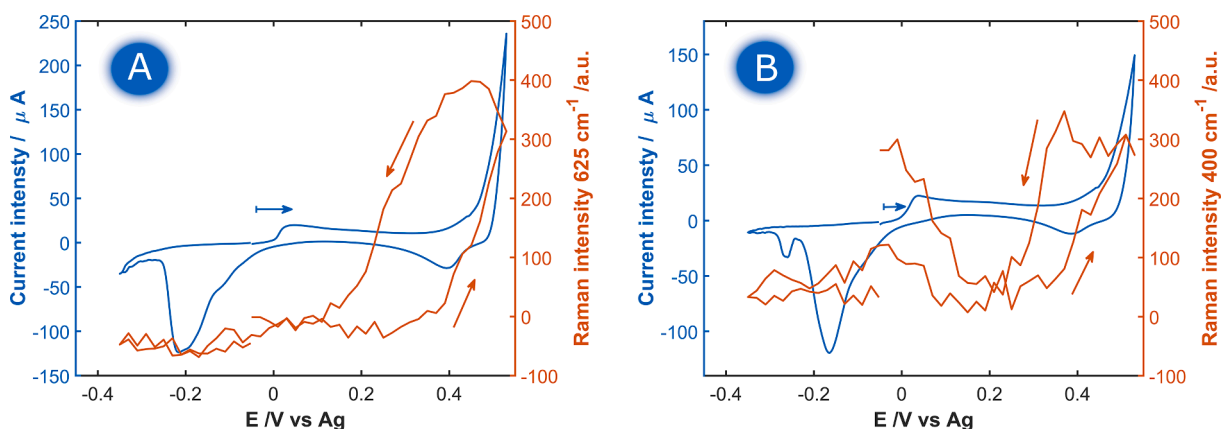
Fig. 4. CV and VoltaRamangram of (A) 625 cm^{-1} Raman band of picloram. (B) 400 cm^{-1} Raman band of 2,4-D. Electrolytic conditions: HClO$_4$ 0.1 M + KBr 5 mM + herbicide 0.1 mM.
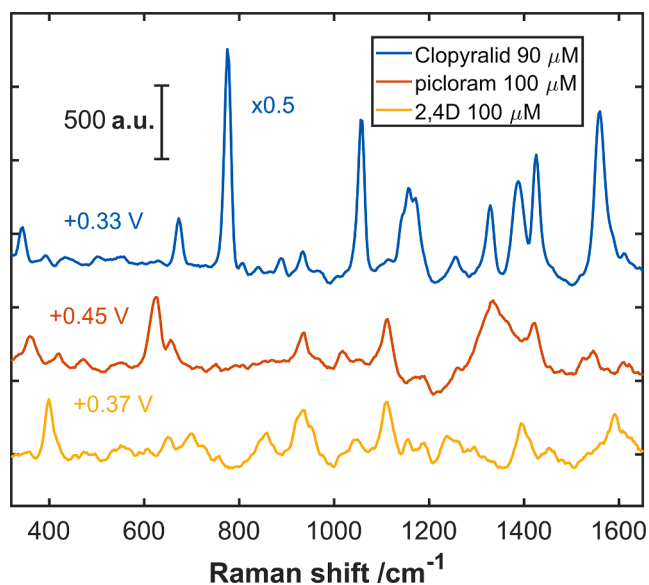
Fig. 5. EC-SOERS spectra of clopyralid, picloram and 2,4-D. Each spectrum was taken at the potential of maximum Raman enhancement. Those potentials are indicated for each spectrum.

response in the vertex potential. For these experiments we found that the Raman intensity is especially reproducible at the anodic vertex potential of the CV, +0.53 V, being this position the one selected for the calibration curve. A tap water test sample was used to demonstrate the good performance of the new methodology: a 45 μM clopyralid solution spiked in tap water containing 5 mM KBr + 0.1 M HClO$_4$ was used without any other treatment. Good figures of merit were obtained for the calibration curve ($I_{Raman, 775 cm}^{-1}$ = 41.8 C$_{clopyralid}$–3.3) shown in Fig. 3B. A good correlation coefficient (R^2 = 0.993) is assessed. A good accuracy is obtained in the prediction, 47 ± 9 μM, 104 % of recovery, with a 7.62 % of relative standard deviation (%RSD) for the determination of clopyralid in tap water, which is a very good value for analytical methods based on Raman spectroscopy.

3.4. Interfering compounds analysis

As was aforementioned, clopyralid is a commonly used herbicide available in different commercial products. Usually, these products contain mixtures of several similar herbicides. One example of this kind of mixtures is the combination of clopyralid and picloram (4-Amino-3,5,6-trichloropyridine-2-carboxylic acid) or clopyralid and 2,4-D (2,4-Dichlorophenoxyacetic acid). Since all of these compounds have relatively high solubility in water (>400 mg/L), they could be present in groundwater. For this reason, an interfering compounds analysis with picloram and 2,4–D was carried out to study the effect of these compounds over the EC-SOERS signal of clopyralid.

One of the great advantages of using EC-SOERS for quantification is the high chemical selectivity of this phenomenon. EC-SOERS is highly selective to molecules containing carbonyls and carboxylates, and because of this, it is possible to perform quantitative analysis in complex matrices without suffering of severe interfering processes, since most of compounds in those matrixes do not show EC-SOERS enhancement during the oxidation of the silver electrode. This fact has been previously demonstrated in the determination of uric acid in synthetic urine [31] and in the determination of vitamin B3 in a multivitamin complex [32]. The main interfering compounds in EC-SOERS tend to be molecules with similar structure to the analyte. In this case, both picloram and 2,4-D show EC-SOERS effect (Fig. 4), due to its great structural similarity with clopyralid.

Another great advantage of Raman spectroscopy is the specific
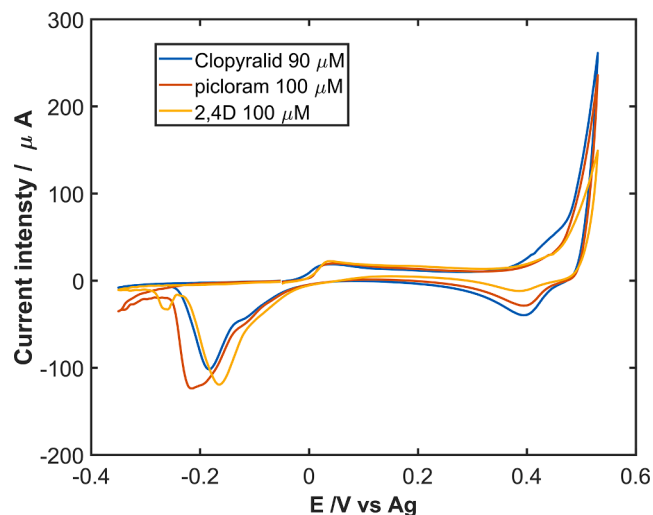
Fig. 6. CVs of a AgSPE in presence of clopyralid, picloram and 2,4-D. Electrolytical conditions: HClO$_4$ 0.1 M + KBr 5 mM + herbicide 0.1 mM.

spectra obtained for the molecules, obtaining chemical fingerprints of the molecules, since several Raman bands can be detected for each analyte. Therefore, spectroscopic signals of different compounds, coexisting in the same sample/spectra, can be analyzed without causing any interference. In our case, as can be observed in Fig. 5, the main Raman band of clopyralid at 775 cm^{-1} is not overlapped by picloram or 2,4-D. This result suggests that the quantification of clopyralid in the presence of these compounds should be possible without suffering any optical interference.

Optical interferences are not the only fact to consider. Unfortunately, the presence of 2,4-D and picloram in the system has an important effect on the electrochemical response of the AgSPE, as shown in Fig. 6, and therefore, on the spectroscopic signal. The presence of these compounds limits the oxidation of the AgSPE to generate Ag$^+$, presumably due to the adsorption of the molecules on the electrode surface. This adsorption results in a smaller current during the dissolution of the electrode, yielding a lower EC-SOERS intensity. Therefore, clopyralid can be studied in presence of 2,4-D and picloram, but the sensitivity of the method decays in presence of these molecules. To solve this problem in a simple way, a standard addition was performed for the quantification of clopyralid in the presence of picloram and 2,4-D, avoiding the prominent matrix effect.

Initially, a water sample spiked with 35 μM clopyralid and 50 μM 2,4-D in 0.1 M HClO$_4$ + 5 mM KBr was used as test sample, increasing the concentrations of clopyralid to perform the standard addition, by doubling the analytical signal of the solution. All samples were analyzed using the spectroelectrochemistry protocol described in section 2.3. Another sample was prepared containing the two interfering compounds, 50 μM 2,4-D and 50 μM picloram, and 35 μM clopyralid, being measured using the same protocol, allowing us to study the influence of several interfering compounds at the same time in the solution. The results of the analysis are summarized in Table 2.

A comparison of the two standard addition models with the univariant calibration shown in Fig. 3 indicates that the studied interfering compounds shows a high influence on the sensitivity of the method, as can be deduced in the evolution of the slopes. The higher the total concentration of 2,4-D and picloram, the lower slope of the calibration curve. This fact could be related to the adsorption of these species on the silver electrode, limiting the anodic dissolution of the electrode (Fig. 6). Nevertheless, clopyralid can be quantified despite this strong effect without using any separation technique and without any pretreatment of the sample.

As usually in standard addition, confidence intervals are wider than in univariate regression because of the position of the test sample

Table 2

Figures of merit of the standard addition performed in the presence of 2,4-D and a mixture of 2,4-D and picloram.

$C_{2,4\text{-}D}$/µM	$C_{picloram}$/µM	$C_{clopyralid}$/µM	Predicted $C_{clopyralid}$/µM	Confidence interval/µM	Slope/µM^{-1}	Intercept/a.u	R^2
50	–	35	34.12 µM	27.90 – 40.34	21.32	727.49	0.999
50	50	35	31.96 µM	12.73 – 51.19	14.75	471.36	0.989

relative to the calibration samples, but in presence of the two interfering compounds, clopyralid is determined without using any separation technique and without any pretreatment of the sample. The confidence intervals for standard addition were calculated by using the interpolation and error propagation method [39,40].

Although the presence of picloram and 2,4-D may decrease the sensitivity of the method, the concentration of these compounds in groundwater is usually lower than that of clopyralid, due to the higher solubility of this molecule. Therefore, the influence of these interfering compounds is expected to be significantly lower in the analysis of real samples. Nevertheless, these problems could be overcome by using multivariate analysis tools, which can assess the influence of interfering compounds on both the spectroscopic signal of clopyralid and the electrochemical signal of the AgSPE oxidation. Due to the correlation between these two factors, this strategy could help us to further develop of the methodology proposed here.

4. Conclusions

A new methodology based on Raman spectroelectrochemistry has been proposed for the first time ever for the detection of clopyralid in aqueous matrices. This methodology is based on the EC-SOERS phenomenon using AgSPE electrodes and it has been demonstrated to be useful for the quantitative analysis of clopyralid in tap water samples. For this purpose, the influence of the precipitating agent used to generate the EC-SOERS substrate has been evaluated, obtaining the optimal conditions to carry out the analysis. The influence of two reasonable interfering compounds (2,4-D and picloram) on the Raman response of clopyralid has been studied, finding that these compounds are adsorbed on the silver electrode surface, limiting the anodic current of the electrochemical oxidation of the silver electrodes. The sensitivity of the analytical method diminishes with the concentration of interfering compounds and a standard addition method is required to determine clopyralid in complex samples. Although this interference should not be important for the analysis of tap water samples, due to the low presence of herbicides, this influence should be considered for the analysis of groundwater, lakes and rivers, where the accumulation of these compounds can be higher. This work reports for the first time the enhancement of the Raman response of clopyralid, presumably due to the difficulty of adsorption of this molecule on metallic substrates by SERS or EC-SERS methodologies. DFT calculations has been carried out to verify that the observed Raman spectrum corresponds to clopyralid, whose Raman spectrum has never been reported. DFT calculations also helped us to propose a tentative Raman band assignment. This study reveals that EC-SOERS is an interesting phenomenon that can be used to study key analytes which are not easily detectable by classical SERS strategies.

Declaration of Competing Interest

The authors declare that they have no known competing financial interests or personal relationships that could have appeared to influence the work reported in this paper.

Data availability

Data will be available at the Universidad de Burgos data repository

Appendix A. Supplementary data

Supplementary data to this article can be found online at https://doi.org/10.1016/j.microc.2022.108018.

References

[1] T.A. Unger, Clopyralid, in: Pestic. Synth. Handb., Elsevier, 1996: p. 530. 10.1016/B978-081551401-5.50415-9.

[2] L. Cox, R. Celis, M.C. Hermosin, J. Cornejo, Leaching patterns of pesticides as related to sorption and porosity properties of soils, Bright. Crop Prot. Conf. - Pests Dis. - 1994, 1-3. (1994) 1325–1330.

[3] P.L. Tomco, K.N. Duddleston, E.J. Schultz, B. Hagedorn, T.J. Stevenson, S.S. Seefeldt, Field degradation of aminopyralid and clopyralid and microbial community response to application in Alaskan soils, Environ. Toxicol. Chem. 35 (2016) 485–493, https://doi.org/10.1002/etc.3222.

[4] M.A. Khan, F.B. Costa, O. Fenton, P. Jordan, C. Fennell, P.E. Mellander, Using a multi-dimensional approach for catchment scale herbicide pollution assessments, Sci. Total Environ. 747 (2020), 141232, https://doi.org/10.1016/j.scitotenv.2020.141232.

[5] X. Li, J. Li, W. Yin, L. Zhang, Clopyralid detection by using a molecularly imprinted electrochemical luminescence sensor based on the "gate-controlled" effect, J. Solid State Electrochem. 18 (2014) 1815–1822, https://doi.org/10.1007/s10008-014-2380-8.

[6] Q. Wang, S. Li, J. Li, A molecularly imprinted sensor with enzymatic enhancement of electrochemiluminescence of quantum dots for ultratrace clopyralid determination, Anal. Bioanal. Chem. 410 (2018) 5165–5172, https://doi.org/10.1007/s00216-018-1170-z.

[7] A. Özcan, M. Gürbüz, Development of a modified electrode by using a nanocomposite containing acid-activated multi-walled carbon nanotube and fumed silica for the voltammetric determination of clopyralid, Sensors Actuators, B Chem. 255 (2018) 262–267, https://doi.org/10.1016/j.snb.2017.08.010.

[8] Y. Tian, X. Liu, F. Dong, J. Xu, C. Lu, Z. Kong, Y. Wang, Y. Zheng, Simultaneous determination of aminopyralid, clopyralid, and picloram residues in vegetables and fruits using ultra-performance liquid chromatography/tandem mass spectrometry, J. AOAC Int. 95 (2012) 554–559, https://doi.org/10.5740/jaoacint.11-120.

[9] S. Tan, H. Yu, Y. He, M. Wang, G. Liu, S. Hong, F. Yan, Y. Wang, M.Q. Wang, T. Li, J. Wang, A.M. Abd EI-Aty, A. Hacımüftüoğlu, Y. She, A dummy molecularly imprinted solid-phase extraction coupled with liquid chromatography-tandem mass spectrometry for selective determination of four pyridine carboxylic acid herbicides in milk, J. Chromatogr. B Anal. Technol. Biomed, Life Sci. 1108 (2019) 65–72.

[10] E. Watanabe, N. Seike, Detection of herbicide clopyralid at nanogram per gram level in agricultural products using easy-to-use micro liquid–liquid extraction followed by analysis with ultraperformance liquid chromatography–tandem mass spectrometry, J. Chromatogr. A. 1630 (2020), 461578, https://doi.org/10.1016/j.chroma.2020.461578.

[11] S. Schütz, H. Vedder, R.-A. Düring, B. Weissbecker, H.E. Hummel, Analysis of the herbicide clopyralid in cultivated soils, J. Chromatogr. A. 754 (1996) 265–271, https://doi.org/10.1016/S0021-9673(96)00156-2.

[12] R. Moldovan, E. Vereshchagina, K. Milenko, B.-C. Iacob, A.E. Bodoki, A. Falamas, N. Tosa, C.M. Muntean, C. Farcău, E. Bodoki, Review on combining surface-enhanced Raman spectroscopy and electrochemistry for analytical applications, Anal. Chim. Acta 1209 (2022) 339250, https://doi.org/10.1016/j.aca.2021.339250.

[13] M. Fleischmann, P.J. Hendra, A.J. McQuillan, Raman spectra of pyridine adsorbed at a silver electrode, Chem. Phys. Lett. 26 (1974) 163–166, https://doi.org/10.1016/0009-2614(74)85388-1.

[14] P.L. Stiles, J.A. Dieringer, N.C. Shah, R.P. Van Duyne, Surface-enhanced Raman spectroscopy, Annu. Rev. Anal. Chem. 1 (2008) 601–626, https://doi.org/10.1146/annurev.anchem.1.031207.112814.

[15] B. Sharma, R.R. Frontiera, A.-I. Henry, E. Ringe, R.P. Van Duyne, SERS: Materials, applications, and the future, Mater. Today 15 (2012) 16–25, https://doi.org/10.1016/S1369-7021(12)70017-2.

[16] G. Demirel, H. Usta, M. Yilmaz, M. Celik, H.A. Alidagi, F. Buyukserin, Surface-enhanced Raman spectroscopy (SERS): An adventure from plasmonic metals to organic semiconductors as SERS platforms, J. Mater. Chem. C. 6 (2018) 5314–5335, https://doi.org/10.1039/c8tc01168k.

[17] D.Y. Wu, J.F. Li, B. Ren, Z.Q. Tian, Electrochemical surface-enhanced Raman spectroscopy of nanostructures, Chem. Soc. Rev. 37 (2008) 1025–1041, https://doi.org/10.1039/b707872m.

[18] S. Schlücker, Surface-enhanced raman spectroscopy: concepts and chemical applications, Angew. Chemie - Int. Ed. 53 (2014) 4756–4795, https://doi.org/10.1002/anie.201205748.

[19] S.-Y. Ding, E.-M. You, Z.-Q. Tian, M. Moskovits, Electromagnetic theories of surface-enhanced Raman spectroscopy, Chem. Soc. Rev. 46 (2017) 4042–4076, https://doi.org/10.1039/C7CS00238F.

[20] K.L. Wustholz, A.-I. Henry, J.M. McMahon, R.G. Freeman, N. Valley, M.E. Piotti, M.J. Natan, G.C. Schatz, R.P. Van Duyne, Structure−Activity relationships in gold nanoparticle dimers and trimers for surface-enhanced raman spectroscopy, J. Am. Chem. Soc. 132 (2010) 10903–10910, https://doi.org/10.1021/ja104174m.

[21] J. Langer, D. Jimenez de Aberasturi, J. Aizpurua, R.A. Alvarez-Puebla, B. Auguié, J.J. Baumberg, G.C. Bazan, S.E.J. Bell, A. Boisen, A.G. Brolo, J. Choo, D. Cialla-May, V. Deckert, L. Fabris, K. Faulds, F.J. García de Abajo, R. Goodacre, D. Graham, A.J. Haes, C.L. Haynes, C. Huck, T. Itoh, M. Käll, J. Kneipp, N.A. Kotov, H. Kuang, E.C. Le Ru, H.K. Lee, J.-F. Li, X.Y. Ling, S.A. Maier, T. Mayerhöfer, M. Moskovits, K. Murakoshi, J.-M. Nam, S. Nie, Y. Ozaki, I. Pastoriza-Santos, J. Perez-Juste, J. Popp, A. Pucci, S. Reich, B. Ren, G.C. Schatz, T. Shegai, S. Schlücker, L.-L. Tay, K.G. Thomas, Z.-Q. Tian, R.P. Van Duyne, T. Vo-Dinh, Y. Wang, K.A. Willets, C. Xu, H. Xu, Y. Xu, Y.S. Yamamoto, B. Zhao, L.M. Liz-Marzán, Present and future of surface-enhanced raman scattering, ACS Nano. 14 (2020) 28–117, https://doi.org/10.1021/acsnano.9b04224.

[22] S.L. Kleinman, B. Sharma, M.G. Blaber, A.-I. Henry, N. Valley, R.G. Freeman, M.J. Natan, G.C. Schatz, R.P. Van Duyne, Structure enhancement factor relationships in single gold nanoantennas by surface-enhanced raman excitation spectroscopy, J. Am. Chem. Soc. 135 (2013) 301–308, https://doi.org/10.1021/ja309300d.

[23] J.R. Lombardi, R.L. Birke, A unified approach to surface-enhanced raman spectroscopy, J. Phys. Chem. C. 112 (2008) 5605–5617, https://doi.org/10.1021/jp800167v.

[24] K. Kneipp, Chemical contribution to SERS enhancement: an experimental study on a series of polymethine dyes on silver nanoaggregates, J. Phys. Chem. C. 120 (2016) 21076–21081, https://doi.org/10.1021/acs.jpcc.6b03785.

[25] M. Yilmaz, E. Babur, M. Ozdemir, R.L. Gieseking, Y. Dede, U. Tamer, G.C. Schatz, A. Facchetti, H. Usta, G. Demirel, Nanostructured organic semiconductor films for molecular detection with surface-enhanced Raman spectroscopy, Nat. Mater. 16 (2017) 918–924, https://doi.org/10.1038/nmat4957.

[26] M. Fan, G.F.S. Andrade, A.G. Brolo, A review on recent advances in the applications of surface-enhanced Raman scattering in analytical chemistry, Anal. Chim. Acta 1097 (2020) 1–29, https://doi.org/10.1016/j.aca.2019.11.049.

[27] D. Martín-Yerga, A. Pérez-Junquera, M.B. González-García, D. Hernández-Santos, P. Fanjul-Bolado, Towards single-molecule in situ electrochemical SERS detection with disposable substrates, Chem. Commun. 54 (2018) 5748–5751, https://doi.org/10.1039/C8CC02069H.

[28] Z.-B. Lin, B.-G. Xie, J.-H. Tian, Y.-A. Tang, J.-J. Sun, G.-N. Chen, B. Ren, B.-W. Mao, Z.-Q. Tian, Potential-dependent adsorption of uracil on a silver electrode in alkaline solutions, J. Electroanal. Chem. 636 (2009) 74–79, https://doi.org/10.1016/j.jelechem.2009.09.014.

[29] J.V. Perales-Rondon, S. Hernandez, D. Martin-Yerga, P. Fanjul-Bolado, A. Heras, A. Colina, Electrochemical surface oxidation enhanced Raman scattering, Electrochim. Acta 282 (2018) 377–383, https://doi.org/10.1016/j.electacta.2018.06.079.

[30] M. Perez-Estebanez, S. Hernandez, J.V. Perales-Rondon, E. Gomez, A. Heras, A. Colina, Chemical selectivity in electrochemical surface oxidation enhanced Raman scattering, Electrochim. Acta 353 (2020), 136560, https://doi.org/10.1016/j.electacta.2020.136560.

[31] S. Hernandez, J.V. Perales-Rondon, A. Heras, A. Colina, Determination of uric acid in synthetic urine by using electrochemical surface oxidation enhanced Raman scattering, Anal. Chim. Acta 1085 (2019) 61–67, https://doi.org/10.1016/j.aca.2019.07.057.

[32] S. Hernandez, J.V. Perales-Rondon, A. Arnaiz, M. Perez-Estebanez, E. Gomez, A. Colina, A. Heras, Determination of nicotinamide in a multivitamin complex by electrochemical-surface enhanced Raman spectroscopy, J. Electroanal. Chem. 879 (2020), 114743, https://doi.org/10.1016/j.jelechem.2020.114743.

[33] A.D. Becke, Density-functional thermochemistry. III. The role of exact exchange, J. Chem. Phys. 98 (1993) 5648–5652, https://doi.org/10.1063/1.464913.

[34] C. Lee, W. Yang, R.G. Parr, Development of the Colle-Salvetti correlation-energy formula into a functional of the electron density, Phys. Rev. B. 37 (1988) 785–789, https://doi.org/10.1103/PhysRevB.37.785.

[35] F. Weigend, R. Ahlrichs, Balanced basis sets of split valence, triple zeta valence and quadruple zeta valence quality for H to Rn: Design and assessment of accuracy, Phys. Chem. Chem. Phys. 7 (2005) 3297, https://doi.org/10.1039/b508541a.

[36] D. Andrae, U. Haussermann, M. Dolg, H. Stoll, H. Preuss, Energy-adjustedab initio pseudopotentials for the second and third row transition elements, Theor. Chim. Acta 77 (1990) 123–141, https://doi.org/10.1007/BF01114537.

[37] D.F. M. J. Frisch, G. W. Trucks, H. B. Schlegel, G. E. Scuseria, M. A. Robb, J. R. Cheeseman, G. Scalmani, V. Barone, B. Mennucci, G. A. Petersson, H. Nakatsuji, M. Caricato, X. Li, H. P. Hratchian, A. F. Izmaylov, J. Bloino, G. Zheng, J. L. Sonnenberg, M. Had, Gaussian 09, Revision D.01., Gaussian, Inc., Wallingford CT. (2013). https://gaussian.com/g09citation/(accessed June 6, 2022).

[38] J.V. Perales-Rondon, S. Hernandez, A. Heras, A. Colina, Effect of chloride and pH on the electrochemical surface oxidation enhanced Raman scattering, Appl. Surf. Sci. 473 (2019) 366–372, https://doi.org/10.1016/j.apsusc.2018.12.148.

[39] D.A. Goncalves, B.T. Jones, G.L. Donati, The reversed-axis method to estimate precision in standard additions analysis, Microchem. J. 124 (2016) 155–158, https://doi.org/10.1016/j.microc.2015.08.006.

[40] G.R. Bruce, P.S. Gill, Estimates of precision in a standard additions analysis, J. Chem. Educ. 76 (1999) 805–807, https://doi.org/10.1021/ed076p805.